Nature and reactivity of the active species formed after NO adsorption and NO + O_2 coadsorption on an Fe-containing zeolite

Andrea R. Beltramone and Oscar A. Anunziata*

Grupo Fisicoquímica de Nuevos Materiales /Centro de Investigación y Tecnología Química (CITeQ), Universidad Tecnológica Nacional, Facultad Regional Córdoba, Maestro Lopez esq. Cruz Roja, s/n, 5016, Córdoba, Argentina

Received 5 September 2003; accepted 14 November 2003

Reactivity of the NO adspecies on Fe-ZSM-11 was studied by FTIR *in situ*. The effect of Fe content and the oxidation state of Fe in the samples were correlated with the catalytic activity. The relation between the adsorbed species, the Brønsted sites and catalytic activity in the SCR of NO_x to N_2 was also investigated. Moreover, FTIR allowed us to identify the active sites and the adsorption complexes present in FeMFI. Samples prepared by the sol–gel method with different Fe content displaying vastly different activity and selectivity in the reduction of NO to N_2 with isobutane in excess of O_2. Thus, in contact with pure nitric oxide, NO ions, mononitrosyl groups, nitro groups and nitrate ions have been identified. Fe^{n+} active sites are the most probable centers for NO oxidation to NO_2 and its further conversion to adsorbed nitro groups and nitrate ions, steps that are crucial for NO reduction. The concerted action of Fe^{n+} and H^+ sites of the catalysts over the NO conversion to N_2 and isobutane conversion was analyzed.

KEY WORDS: NO adsorption; FTIR; intermediate species, Fe-ZSM-11.

1. Introduction

Selective catalytic reduction (SCR) of NO by hydrocarbons is a very important field of environmental catalysis research. The use of catalysts, including noble metals (e.g. Pt, Pd, Rh), reduces considerably the environmental problems caused by unburned and partially oxidized hydrocarbons, carbon monoxide and nitrogen oxides in exhaust gas purification. The harmful emissions are converted to less hazardous compounds like N_2, CO_2 and H_2O with the help of a catalyst. NO reduction reactions on the catalyst surface are very complex. Research groups in industry and at universities have shown a lot of interest in investigating the possible reaction mechanisms. Many research groups have used FTIR spectroscopy to investigate the reaction intermediates in NO reduction by hydrocarbons, like CH_4 and C_3H_6 [1–6], CO [7–8] and H_2 [9] over different catalysts.

Zeolite MFI supported iron catalysts have recently attracted considerable attention. At low iron loading, Fe/MFI has been reported to be active for the partial oxidation of benzene to phenol and of methane to methanol with N_2O as the oxidant [10]. With high iron loadings, certain over-exchanged Fe/MFI catalysts have demonstrated high activity and remarkable stability for the selective catalytic reduction SCR of NO by hydrocarbons in the presence of a large excess of oxygen and water vapor. As to the nature of the active sites, binuclear iron complexes have been proposed by several researchers [11–12]. The performance of metal-exchanged ZSM-5 catalysts for the reduction of NO by hydrocarbons in the presence of excess O_2 is generally inhibited by the presence of water. It has been determined recently, however, that Fe exchanged into ZSM-5 is active for NO reduction by isobutane in the presence of H_2O vapor at concentrations as high as 20% [13–16]. The preparation of Fe–ZSM-5 with a high loading of iron has proven to be a challenge. While Feng and Hall [13–14] reported that a Fe/Al ratio of up to 0.93 could be achieved by ion exchange of Na–ZSM-5 using a saturated aqueous solution of ferrous oxalate [13–14], attempts by Chen and Sachtler [15–16] to use this procedure were unsuccessful in achieving such high exchange levels. Moreover, these latter authors noted that differences in catalyst performance were observed, which appeared to be related to subtle differences in zeolite history. Reproducible performance could be achieved, though, using dry exchange of H–ZSM-5 with $FeCl_3$. In a related study, ion exchange with $Fe(NO_3)_3$ was carried out with ZSM-5 [17].Only limited characterization of Fe–ZSM-5 has been reported to date.

Evidence for nanoclusters of iron oxide obtained by EXAFS has been reported, though, for Fe–ZSM-5 prepared by aqueous ion exchange from ferric nitrate [17].

In Fe/MFI with low iron loading, Panov *et al.* [10–12], Sobolev *et al.* [18–19] and Ovanesyan *et al.* [20] found that a particular state of adsorbed oxygen, called

---

* To whom correspondence should be addressed.
E-mail: Oanuziata@scdt.frc.utn.edu.ar

1011-372X/04/0200–0131/0 © 2004 Plenum Publishing Corporation

α-oxygen, is important. They believe that this α-oxygen is associated with binuclear Fe complexes. For over-exchanged Fe/MFI, Feng and Hall [21] and Sachtler *et al.* [22] have suggested that two iron ions are involved in a redox cycle during the SCR of NO. An oxygen-bridged binuclear iron complex HO–Fe–O–Fe–OH was proposed by Sachtler [22]. This model permits a simple rationalization of the H-TPR and CO-TPR data and correctly describes the maximum metal loading with $Fe/Al = 1$. It also explains the thermal reduction behavior, as the bridging oxygen can be thought to be desorbed, thus reducing the two iron ions from Fe^{+3} to Fe^{+2}. Desorption of oxygen from Fe/MFI prepared by hydrothermal synthesis was observed by Lazar *et al.* [23], who also proposed an Fe–O–Fe pair as the redox center. Other models of the active sites in Fe/MFI catalysts for the SCR of NO have also been proponed by Kucherov *et al.* [24], who quote ESR evidence, and by Lee and Rhee [25], who considered isolated Fe ions as active sites. Joyner and Stockenhuber [26] did extended X-ray absorption fine structure (EXAFS) work on catalysts of low SCR activity and proposed Fe_4O_4 nanoclusters as active sites, while conceding, however, that the state of the iron will strongly depend on the preparation method. Sachtler *et al.* [22] developed a sublimation method to prepare Fe/MFI with high iron loading and high SCR activity. The iron ions are found to be homogeneously distributed inside the zeolite cavities, compensating the negative charge of the zeolite framework, though part of the ions appear as aggregate forming microscopic rafts of iron oxide on the zeolite support. A treatment with an aqueous NaOH solution transforms iron ions in Fe/MFI to larger aggregates, which appear as iron oxide clusters after calcination. These clusters are still located inside zeolite channels [27]. Catalytic tests show that iron oxide clusters have low activity for the SCR of NO. Two issues requiring further clarification are the precise nature of the sites and the mechanism by which NO complexes are formed.

In our previous works [28–29], Fe-ZSM-11 zeolite was prepared by a novel sol–gel process with Fe^{2+} and/or Fe^{3+} as active sites incorporated by reproducible postsynthesis methods and characterized by XRD, BET and FTIR. These methods confirm the tetragonal symmetry of the synthesized material and their good crystallinity characteristic of MEL-phase. The presence of Fe^{n+} species in Fe-containing zeolite were determined and quantified considering the Fe K-edge shift. Their symmetry and electronic characteristics and the analysis of Fe species are also discussed, employing extended X-ray absorption fine structure (XAFS) spectroscopy. Fe^{2+}, Fe^{3+} and Fe_2O_3 as isolated species and highly dispersed were found as active sites of the material. Investigations of the Electron–Donor–Acceptor (EDA) sites from Fe^{n+} silicates by *in situ* infrared spectroscopy using pyridine as a probe molecule led to the conclusion that the NO_x activity is a function of Fe^{2+} species. Fe^{n+} as counterions generates new Lewis sites. We differentiated it from the well-known Lewis sites from Aluminum in the zeolitic framework. Thus, LUMO (lower unoccupied molecular orbital) of Fe^{n+} and its interaction with the reactant through EDA adduct led to a coordinative activity with Brønsted acid sites, being successfully applicable to the SCR reaction of NO_x. Fe^{+3} species are less active for the SCR of NO_x with isobutane and oxygen, but they show a low selectivity to N_2O. The active species (both, Fe^{2+} and Fe^{3+}) are highly dispersed on the catalyst. According to our results, the performance of Fe-zeolites thereby come up with even better catalyst formulations and could be obtained using the ZSM-11 zeolite with $Fe^{2+}/Al = 0.202$ and $Fe^{3+}/Al = 0.378$ and Brønsted / Lewis sites ratio = 0.6, leading to a good activity and very low selectivity to N_2O [28–29].

In the present work, FTIR of NO adsorption has been used to identify through the intermediate N_xO_y adspecies the nature of the iron sites over Fe/MEL, since several different iron components will actually coexist in this catalyst. The adsorption of NO on these catalysts was followed by FTIR to identify the activity of each iron component. A relationship between the iron sites and Brønsted sites and their catalytic activities will be suggested.

2. Experimental

2.1. Sample preparation

2.1.1. Na zeolites

Na-ZSM11 zeolites were obtained by a novel sol–gel process. The samples were prepared using the following reactants: tetraethylorthosilicate, as the source of silicon; sodium aluminate as the aluminum source and tetrapropylammonium hydroxide as the template. The technique procedure is described by the following steps:

Step (a): TEOS was hydrolyzed with HCl for 1 h and Al source in water were added to the resultant solution at 0 °C. The clear solution obtained was stirred for 20 min.

Step (b): The final solution of step (a) is converted into a solid co-gel by addition of the corresponding template at room temperature. The xerogel obtained was dried at 110 °C overnight.

Step (c): The xerogel obtained in step (b) was impregnated with the adequate template solution by wetness impregnation method. The impregnated SiO_2/Al_2O_3 was charged in a Teflon-lined autoclave and crystallized at 150–180 °C for 56–100 h. The final product was filtered, washed with distilled water, dried at 110 °C and heated for 12 h under nitrogen flow of 10 mL/min and 2 °C/min from 100 to 500 °C, then the samples were calcined in air at 500 °C for 8 h.

2.1.2. Fe^{+2} *and* Fe^{+3} *zeolites*

The ammonium form of the catalyst was prepared by ion exchange of Na zeolites with ammonium chloride 1 M at 80 °C for 40 h. Fe^{+2}-ZSM and Fe^{+3}-ZSM samples were prepared using NH_4 zeolites by wetness impregnation with $FeSO_4 \cdot 7H_2O$ or Fe $(NO_3)_3 \cdot 9H_2O$ solution, using an rotator evaporator allowing us to obtain more uniform Fe-species distribution. The final product was dried at 110 °C and heated for 10 h under nitrogen flow of 10 mL/min and 2 °C/min from 100 to 500 °C and then the samples were calcined in air at 500 °C for 12 h.

The samples under study were denoted as follows: sample A: Fe^{2+}-HZSM-11 (1 wt% Fe^{+2}); sample B: Fe^{2+}-HZSM-11(3 wt% $Fe^{+2,+3}$); sample C: Fe^{3+}-HZSM-11(3 wt% Fe^{+3}). A summary of catalyst characterization is shown in table 1.

2.2. FTIR studies

Infrared measurements were performed on a JASCO 5300 FTIR spectrometer. For structure characterization, the samples were mixed with KBr and pressed forming a wafer. The IR spectra of the catalyst in the region of 1400–400 cm^{-1} (not shown in this paper) indicates that all the samples have good crystallinity taking into account the ratio of the intensity at 550/450 cm^{-1}, characteristic of MEL-phase. For the Fe-containing zeolites the spectra do not show any alteration from the mother samples indicating that the Fe species are not in framework positions. NO adsorption experiments over Fe-H-ZSM11 samples were carried out using a thermostatized cell with CaF_2 windows connected to a vacuum line, with a self-supported wafer. Typically, the samples were pretreated up to 500 °C under flow of O_2 overnight. For NO adsorption, the samples were purged in vacuum for 6 h before 50 torr of NO was introduced into the cell. All spectra were recorded at room temperature as a function of exposure time. For the quantitative comparison of absorbance, we took the absolute value of absorbance per milligram of sample of different wavenumbers. These values were obtained from the FTIR spectra. A reference spectrum of the sample before exposure of NO was subtracted from each spectrum.

2.3. Catalytic experiments

Catalytic activity measurements were conducted in a 1.25-cm o.d. quartz tube reactor in a microcatalytic system. 200 mg of powder catalysts were loaded between two plugs of either silane-treated glass or quartz wool. The reaction temperature was monitored by two chromel–alumel thermocouples, one placed in contact with the outer wall of the quartz reactor next to the catalyst, while the other was placed in the reactor in direct contact with the catalyst powder. The reactor temperature was controlled by varying the power output to the furnace through an Omega CN-2010 programmable temperature controller connected to the first thermocouple. All the gases used in the studied reaction were of ultrahigh purity (UHP) grade, obtained from Sooner Airgas and used as were received. Inlet reactant feed was composed of 400 ppm NO/He, 5000 ppm i-C4H10/He, 5% O_2 balanced with He. Gaseous flow rates of 100 cm^3/ min were independently controlled by individual Porter mass flow meters. Prior to activity measurements, catalysts were pretreated *in situ* by heating under He flow with a ramp of 4 °C/min to 500 °C and held at 500 °C for 1 h, thereafter cooled to desired temperature. The products and reactants were analyzed on-line. The concentration of NO and NO_2 (i.e. NO_x), and of N_2O were measured using a Thermo Environment High-Level analyzer (42C and 46C). The concentration of i-C4H10/He was determined by using a HP 5890 gas chromatograph (GC), equipped with a FID detector. Products and reactants were injected into a GC from a Valco sampling valve, controlled by a digital sequence programmer with an air actuator every 20 min using a 30-m Molsieve 5A capillary column (Altech, Inc.).

3. Results and discussion

3.1. Adsorption of nitrogen monoxide at room temperature

The adsorption of NO over these catalysts was performed at room temperature with pure NO for 15 min followed by purging with vacuum at 10^{-1} torr.

Table 1
Summary of catalyst characterization

Catalysts	Si/Al[a]	Fe/Al[a]	Fe (wt%)[b]	Fe^{2+}/uc[c]	Fe^{3+}/uc[c]	Brønsted Sites[d]		Lewis Sites[d]	
						350 °C	400 °C	350 °C	400 °C
Sample A	16.9	0.19	1	0.639	0.392	0.058	0.046	0.065	0.045
Sample B	16	0.58	3	1.083	2.018	0.076	0.061	0.115	0.106
Sample C	16	0.58	3	–	3.095	0.084	0.071	0.099	0.087

[a] As made, mole ratio determined by ICP analysis.
[b] wt% by ICP analysis.
[c] XANES analysis [29].
[d] FTIR, pyridine mmol/g retained at different temperatures before desorption at 10^{-4} torr for 6 h.

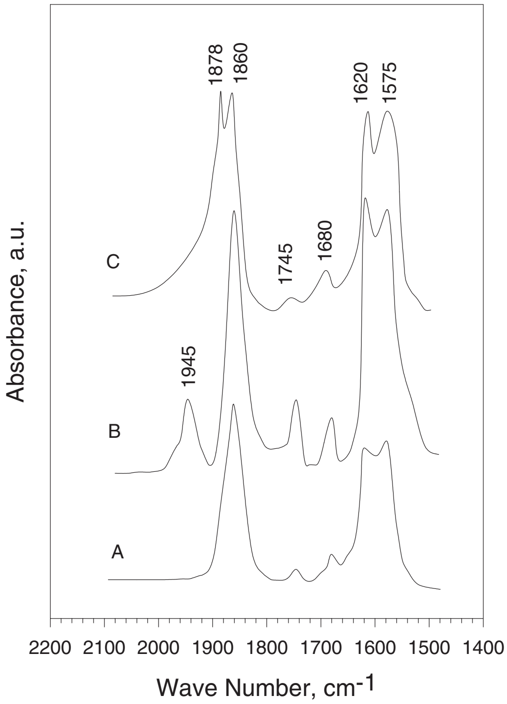

Figure 1. FTIR spectra of NO adsorbed (50 torr equilibrium pressure at 25 °C for 15 min, evacuated in vacuum for 5 min) on Fe-ZSM-11. A: Fe^{2+}-HZSM-11 (1 wt% Fe^{+2}); B: Fe^{2+}-HZSM-11(3 wt% $Fe^{+2,+3}$); C: Fe^{3+}-HZSM-11(3 wt% Fe^{+3}).

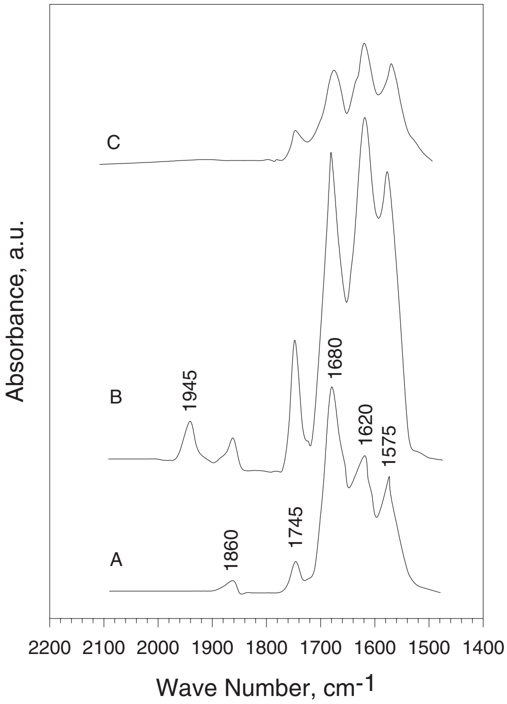

Figure 2. FTIR spectra of NO adsorbed (200 torr equilibrium pressure at 25 °C for 15 min, evacuated with Helium to 760 torr) on Fe-ZSM-11 A: Fe^{2+}-HZSM-11 (1 wt% Fe^{+2}); B: Fe^{2+}-HZSM-11(3 wt% $Fe^{+2,+3}$); C: Fe^{3+}-HZSM-11(3 wt% Fe^{+3}).

From the IR spectra of Fe-ZSM-11 shown in figure 1, when NO was introduced to the samples, two strong peaks were observed at 1860 and 1878 cm^{-1} (this band is close to the vibration frequency of gas-phase NO, 1880 cm^{-1}) and have been assigned to Fe^{+2} or Fe^{+3} mononitrosyls (Fe^{+n} (NO)) [30]. Both bands appear only in sample C on different exchanges sites of Fe^{+3}. Since the position of 1860 cm^{-1} band is the same as that in all samples, Segawa *et al.* [31] found that the position of this band is rather insensitive to the valence state of the iron, rather, it depends on the localization of the Fe ions.

The band at 1745 cm^{-1} can be assigned to N_2O_4; this dimer exists in equilibrium with NO_2 and represents an important component of the gas phase at moderate temperatures. The band at 1945 cm^{-1} in sample B is attributed to NO_2^+ nitrosyl adspecies [32]. NO is adsorbed strongly over Fe^{+2} and Fe^{+3} species, when these are present as counterions, indicating the presence of these isolated species in all the samples. The bands in the range of 1620 and 1575 cm^{-1} are assigned to nitro and nitrate species adsorbed over $Fe^{+2,+3}$ sites [32–34] and the peak at 1680 cm^{-1} is probably due to adsorbed N_2O_3 species since it is close to the IR band at 1690 cm^{-1} for gaseous N_2O_3 [34]. The bands at 1878, 1860 and 1745 cm^{-1} are formed quickly upon exposure to NO; the last bands appear on the three samples, but with different intensity depending on the amount of Fe [30].

Interestingly, all the bands (except 1878 cm^{-1}) appear on the three samples in the same positions, but with different intensity. Figure 1 shows that in sample B the bands at 1860 and 1745 cm^{-1} are more intense, indicating that NO is better adsorbed on Fe^{+2} than Fe^{+3} sites. After the NO-treated samples were purged with Helium to atmospheric pressure, these bands almost decreased sharply or disappeared (figure 2). The peaks at 1620 and 1575 cm^{-1} assigned above to adsorbed NO_2 and NO_3^- species respectively, and the increase of the band at 1680 cm^{-1} can be observed in figure 2. This suggests that NO molecules are weakly adsorbed and that some of them were oxidized to NO_2, N_2O_3 and nitrate species by the residual O_2 species weakly adsorbed on the catalyst. Oxygen improved NO adsorption, clearly because of oxidation of NO to NO_2 and nitrate species. The higher intensity of these bands was observed in the spectrum of sample B in concordance with the higher Fe^{+2} content of this sample.

After the Fe-ZSM-11 samples were purged in vacuum (10^{-2} torr) for 30 min (figure 3), only the 1680, 1620 and 1575 cm^{-1} bands are present, indicating that these species are responsible for the activity of SCR of the NO_x reaction. The comparison between the intensities of the bands for the three samples can be seen in figure 4. The chemisorbed species are higher in sample B in concordance with its catalytic activity (table 2).

When the samples were heated to 100, 200 and 350 °C (figures 5, 6 and 7), the band at 1680 cm^{-1} either decreased sharply or disappeared, while the bands at

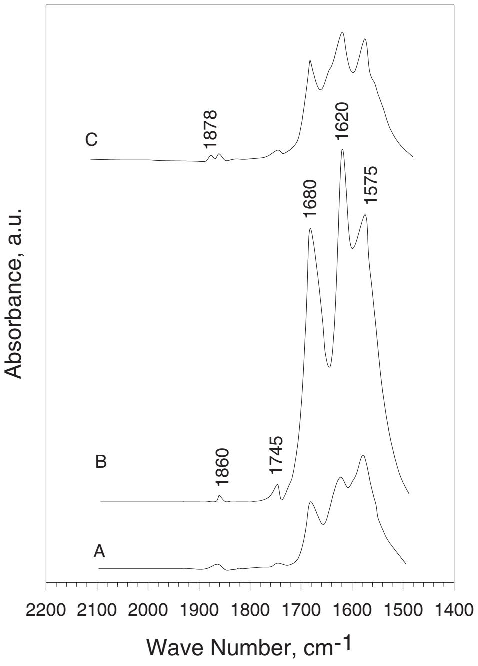

Figure 3. FTIR spectra of NO adsorbed (200 torr equilibrium pressure at 25 °C for 15 min, evacuated in vacuum for 30 min) on Fe-ZSM-11 (A: Fe^{2+}-HZSM-11 (1 wt% Fe^{+2}); B: Fe^{2+}-HZSM-11(3 wt% $Fe^{+2,+3}$; C: Fe^{3+}-HZSM-11(3 wt% Fe^{+3})).

1620 and 1575 cm^{-1} (due to NO_2 and NO_3^- adspecies) remain in the spectrum. As the temperature was further increased, the last bands also decreased at 350 °C. In figure 8, we can see the absorbance (in A units) of the bands versus desorption temperature for the samples A, B and C. According to our experimental results, the NO_2 and NO_3^- adspecies showed a diminution with the desorption temperature. In all the samples the [NO_2—Fe^{+n}] specie band is more intense than the other bands. The intensity of the band at 1680 cm^{-1} assigned above decreases sharply, suggesting that N_2O_3 is desorbed or transformed to NO_2 adspecies. This band is higher for sample B than for the other samples. The 1575 and 1620 cm^{-1} bands are present in much higher extent in sample B than in A and C, according to the quantity of active sites of Fe^{+2} present in the different samples.

3.2. *Adsorption of nitrogen monoxide at* 350 °C

The results of the adsorption of NO (200 torr, followed by 30-min evacuation in vacuum at 10^{-2} torr) at 350 °C on the samples A, B and C are shown in figures 5(e), 6(e) and 7(e). We can observe that the higher intensity bands are present in sample B, so sample B has higher amount of intermediate adspecies for SCR reaction. According to the data of absorbance from the spectra at room temperature and at 350 °C (figure 4(c) and 9), we can observe lower intensity bands in the spectra for NO adsorption at 350 °C than at 25 °C in all the samples. It is interesting to note that the

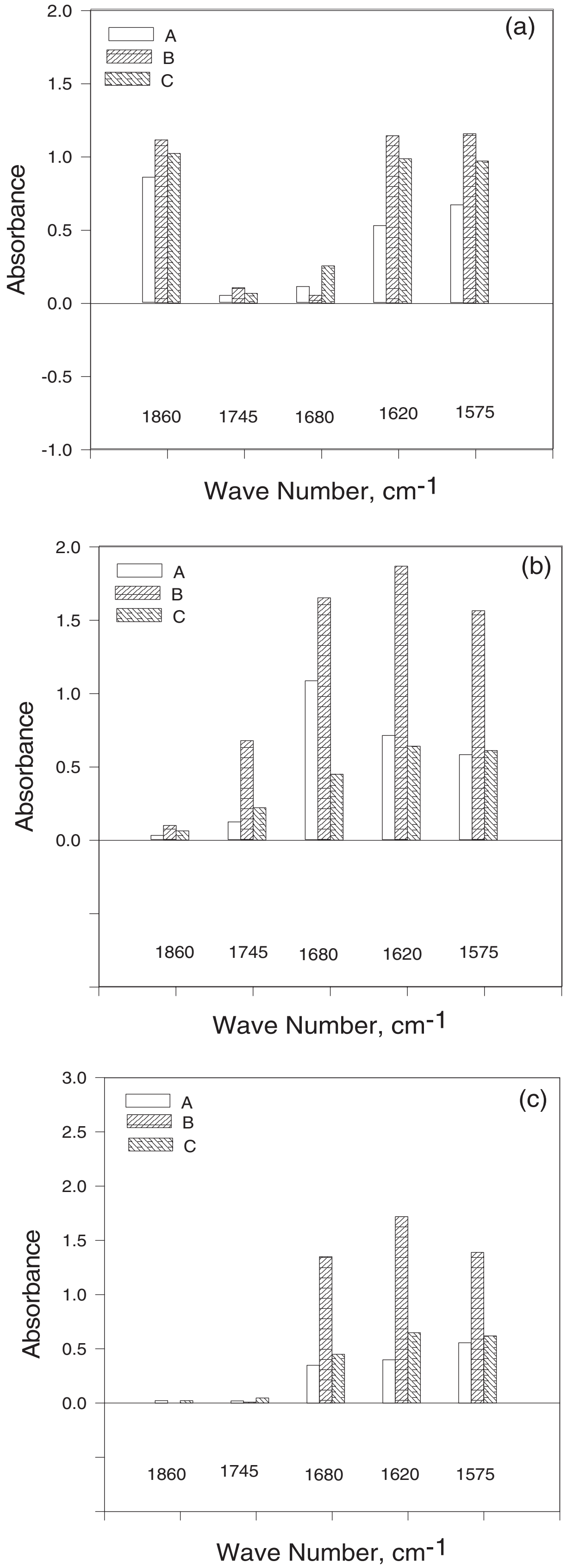

Figure 4. Adsorption of NO over Fe-ZSM-11 samples A, B and C at 25 °C (a) 50 torr for 15 min, evacuated in vacuum for 5 min, (b) 200 torr for 15 min, evacuated with He and (c) 200 torr for 15 min, evacuated in vacuum for 30 min.

Table 2
Catalytic activity at different reaction temperatures; 400 ppm NO/He, 5000 ppm i-C_4H_{10}/He, 5% O_2 balanced with He

Sample	A	B	C	A	B	C
	NO conversion to N_2 (mol%)			isobutane conversion (mol%)		
Temperature (°C)						
350	34	65	20	13.3	42	6.5
400	58	58	25	59.5	80	30
450	62	50	25	70.6	87	55
500	52	46	27	75	90	66

intensity of the bands is higher when the samples are adsorbed at 350 °C than when they are desorbed in vacuum at the same temperature. Figure 9 indicates that the bands assigned to these adspecies are present even at the reaction temperature (350–450 °C), indicating that NO_2 and NO_3^- adspecies might play an important role in the SCR of NO_x over Fe-containing zeolite, in agreement with Sachtler *et al.* [30].

3.3. Relationship between catalytic activity and active sites

In order to analyze the relation of the catalyst activity and the nature of active sites, the changes of catalytic properties coming from the modification of the reaction temperature, are shown in table 2.

With the objective to analyze the concerted action of Fe^{n+} and H^+ sites of the catalysts, we show in figure 10, the NO conversion to N_2 and isobutane conversion (at highest NO conversion at 350 °C, according to the data of table 2) as a function of the absorbance values of $-NO_2$ and $-NO_3^-$ species obtained from the data shown in figure 9 for each sample. The graph shows that the NO and isobutane conversion is indeed highest over sample B, according to the highest value of both the absorption bands ($-NO_2$ and $-NO_3^-$). The first interesting result shown in figure 10 is that the NO conversion and isobutane conversion increase more quickly as a function of the increase of the band attributed to $-NO_3^-$ adspecies than the $-NO_2$ one. We suggest the possible concerted action of NO_y-M (M, metal) adsorbed species and Brønsted acid sites of the samples. So, we choose the absorbance values at 1575 cm^{-1} (NO_3^--M species) and the Brønsted sites (in mmol/g of pyridine retained at 350 °C and 10^{-4} torr at 1554 cm^{-1}, which indicate the PyH^+ sites, see table 1) for each sample to determine the possible relation with NO and isobutane conversion. The results are shown in

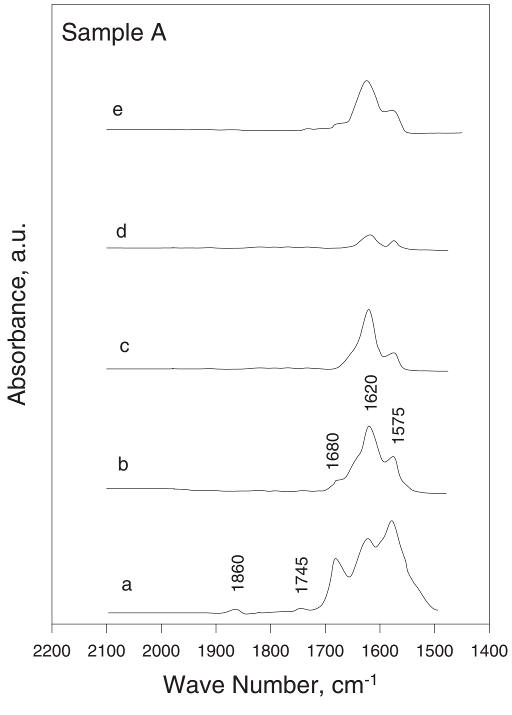

Figure 5. FTIR spectra of NO (200 torr) adsorbed on sample A. (a) Adsorbed at 25 °C, (b) desorbed at 100 °C, (c) desorbed at 200 °C, (d) desorbed at 350 °C and (e) adsorbed at 350 °C.

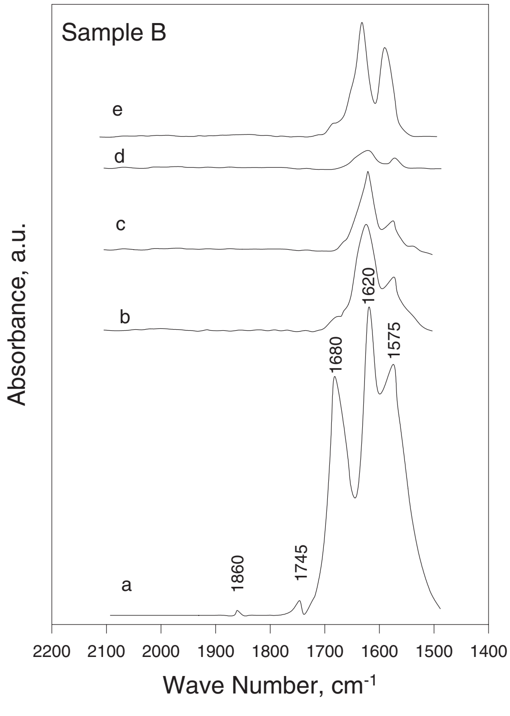

Figure 6. FTIR spectra of NO (200 torr) adsorbed on sample B. (a) Adsorbed at 25 °C, (b) desorbed at 100 °C, (c) desorbed at 200 °C, (d) desorbed at 350 °C and (e) adsorbed at 350 °C.

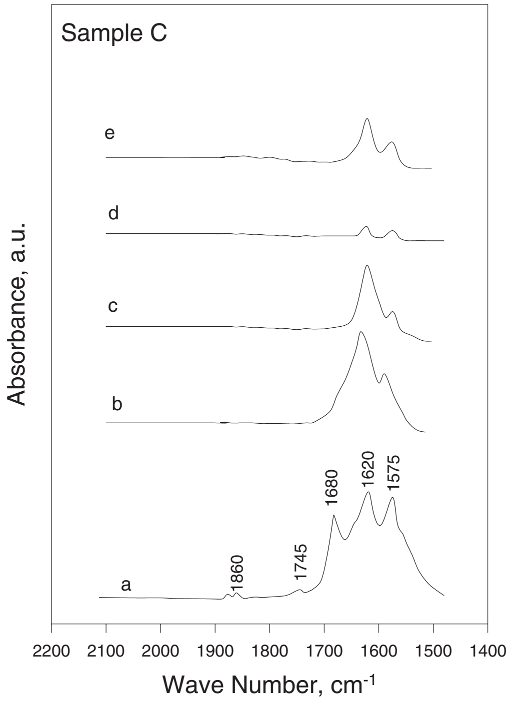

Figure 7. FTIR spectra of NO (200 torr) adsorbed on sample C. (a) Adsorbed at 25 °C, (b) desorbed at 100 °C, (c) desorbed at 200 °C, (d) desorbed at 350 °C and (e) adsorbed at 350 °C.

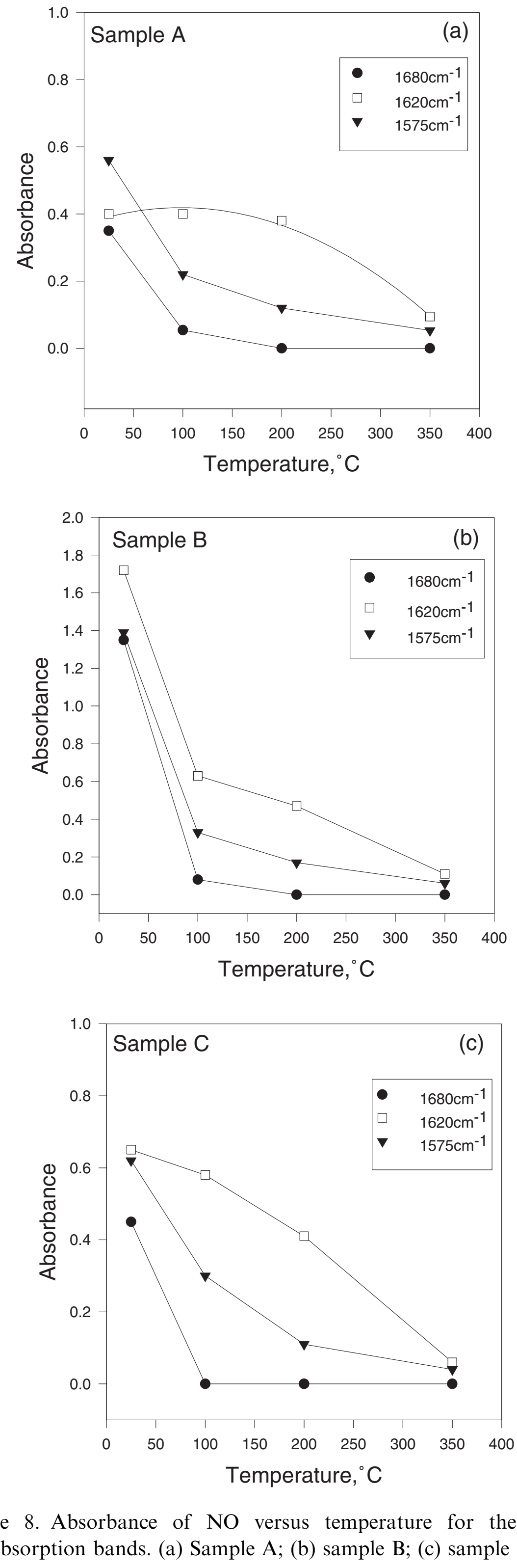

Figure 8. Absorbance of NO versus temperature for the three absorption bands. (a) Sample A; (b) sample B; (c) sample C.

figures 11 and 12. We arrive at the first suggestion: the concerted action of the Brønsted sites and NO_3^- adspecies (preferably on Fe^{2+} sites) in the overall SCR of NO to N_2 in the presence of isobutane and O_2 in excess. According to figures 11 and 12, the highest NO and isobutane conversion is reached when the highest absorbance value of NO_3^-–M specie is present (sample B). The reduction to N_2 is arrived on Brønsted sites in a concerted action with the oxidation of isobutane. Sample C, which possesses the highest number of Brønsted sites, is not a more active sample either to NO conversion or to isobutane conversion (at 350 °C). The first step seems to be the oxidation of NO to NO_2 or NO_3^- and its adsorption as –M reactive specie, and then, this specie is reduced to N_2 over H^+ sites in a nearly geometrical environment. Thus, it is not sufficient that the catalyst has a moderate NO_3^- adspecie quantity if it possesses a low quantity of H^+ sites (see sample A). In the same way, it is also not sufficient that the sample possesses high number of Brønsted acid sites if it does not possess reactive NO_3^- adspecie (see sample C). On the other hand, according to the data shown in table 2, as the temperature increases (> 350 °C), the NO and isobutane conversion decreases for sample B. The maximum of NO and isobutane conversion is found for sample A at 450 °C, according to its minor quantity of NO_3^- adspecie and consequently its highest activation energy for the reaction. For sample C, the few NO_3^- –M species are desorbed and NO conversion is low at all the reaction temperatures studied. Moreover, isobutane conversion increases with the reaction temperature (< 350 °C), but the NO conversion is constant. Isobutene is converted to CO and CO_2 over H^+ sites, but it is not consumed to reduce NO at this temperature (see table 2). At 400 °C, the NO_x conversion to N_2 for samples A and B are similar, but the isobutane

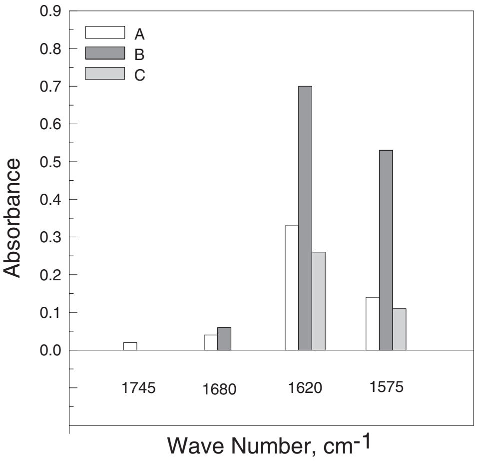

Figure 9. Adsorption of NO at 350 °C on Fe-ZSM-11, samples A, B and C.

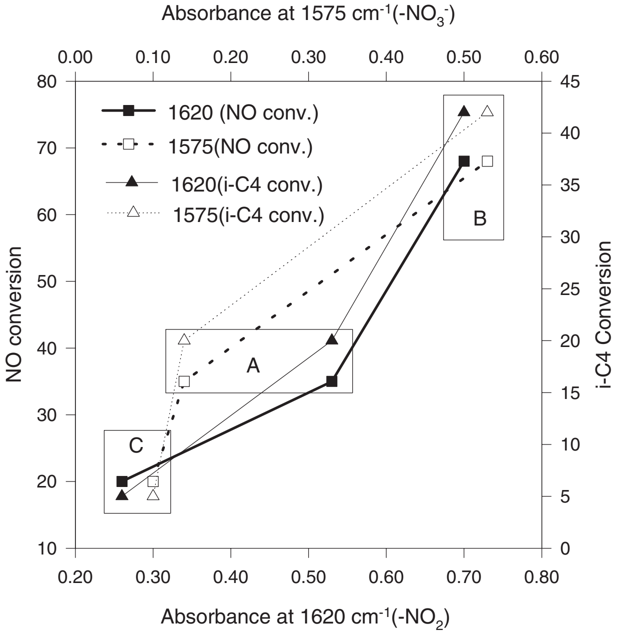

Figure 10. Relationship between the adsorbed species at 350 °C and NO_x and isobutane conversion at 350 °C, for samples A, B and C.

conversion is much higher for sample B than for sample A. In figures 13 and 14, we show the NO_x and isobutane conversion to Brønsted acid sites (retained Py as PyH^+ at 400 °C) and the absorbance value for the band at $1575\,cm^{-1}$. As can be seen, although sample B possesses more NO_3^- adspecie than sample A, the isobutane is converted to CO and CO_2, competing with the reduction of the NO_3^- adspecie, diminishing the overall NO_x conversion to N_2 with respect to the lower reaction temperature (i.e. 350 °C). For sample A, at 400 °C, the NO_x conversion is quite similar to sample B. We must take into account that at this temperature, sample A transforms selectively NO_3^- adspecie to N_2 by its reduction with isobutane, which is not transformed to CO and CO_2 as occurs for the sample B. The SCR of

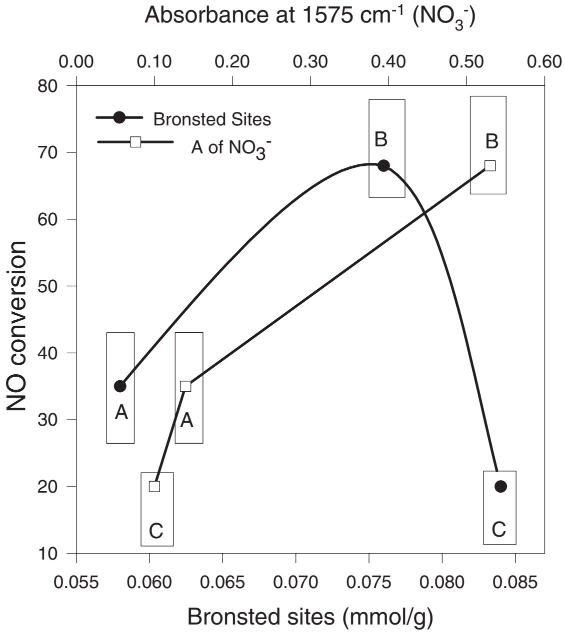

Figure 11. Relationship between NO conversion (mol%) at 350 °C and ($–NO_3^-$) adsorbed specie and Brønsted sites for samples A, B and C.

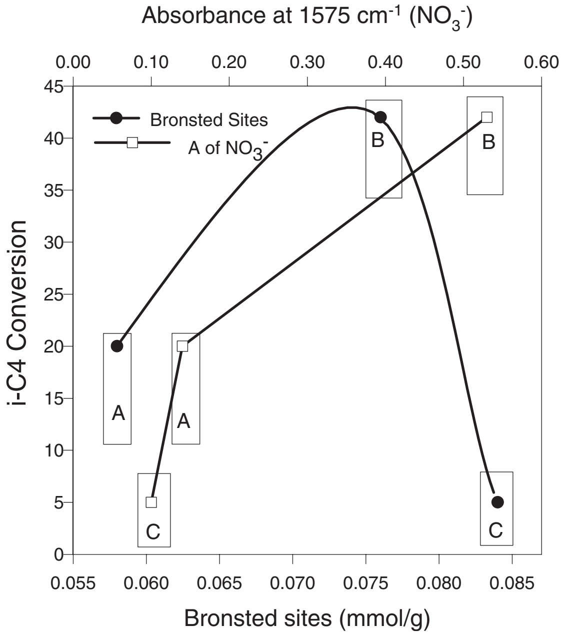

Figure 12. Relationship between isobutane conversion (mol%) at 350 °C and ($–NO_3^-$) adsorbed specie and Brønsted sites for samples A, B and C.

NO do not take place for the samples B and C at reaction temperatures ≫ 450 °C.

4. Conclusions

A detailed *in situ* FTIR investigation undertaken on the adsorption of NO over Fe-containing zeolites indicated the formation of various NO species or complexes with cationic Lewis acid and/or active metal

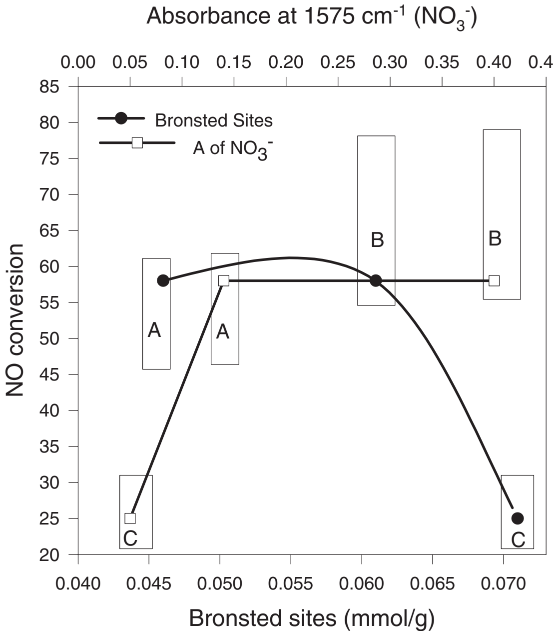

Figure 13. Relationship between NO_x conversion (mol%) at 400 °C and ($–NO_3^-$) adsorbed specie and Brønsted sites for samples A, B and C.

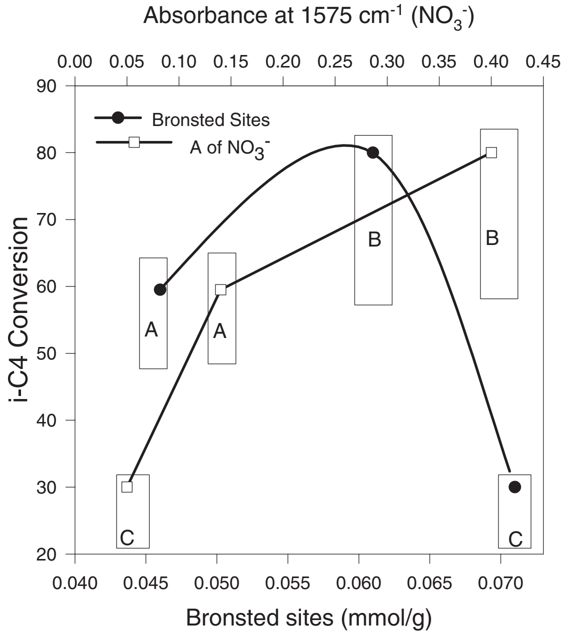

Figure 14. Relationship between isobutane conversion (mol%) at 400 °C and ($–NO_3^-$) adsorbed specie and Brønsted sites for samples A, B and C.

sites. NO adsorption at room temperature and at 350 °C leads to the formation of bands attributed to chemisorbed nitrogen dioxide (NO_2), nitrite ($M–NO_2^-$), nitrate ($M–NO_3^-$) and mononitrosyl (M –NO). Nitrite and nitrate are the most important intermediates for SCR reaction. NO_x reduction probably takes place on the Brønsted acid sites and the role of Fe^{n+} sites is to oxidize NO to NO_2 by O_2.

NO is better adsorbed on Fe^{+2} than Fe^{+3} sites, so sample B has a higher quantity of adsorbed intermediates and Brønsted sites compared to the other samples. Sample B is the most active for this reaction because of the concerted action of the Brønsted sites and NO_3^- adspecies (preferably on Fe^{2+} sites) in the overall SCR of NO to N_2 in the presence of isobutane and O_2 in excess.

Acknowledgments

Oscar A. Anunziata, L.B.P. and Andrea R. Beltramone are grateful to CONICET of Argentina for financial support of their research. The Research was also partially supported by Agencia Córdoba Ciencia grant, PID/2001-2005

References

[1] R. Burch and A. Ramli, Appl. Catal., B 15 (1998) 49.
[2] G.R. Bamwenda, A. Ogata, A. Obuchi, J. Oi, K. Mizuno and J. Skrzypek, Appl. Catal., B 6 (1995) 311.
[3] V. Ermini, E. Finoccio, S. Sechi, G. Busca and S. Rossini, Appl. Catal., A 190 (2000) 157.
[4] K.I. Shimizu, H. Kawabata, A. Satsuma and T. Hattori, Appl. Catal., B 19 (1998) L87.
[5] F.C. Meunier, J.P. Breen, V. Zuzaniuk, M. Olsson and J.R.H. Ross, J. Catal. 187 (1999) 493.
[6] M. Huuhtanen, Master's Thesis (University of Oulu, Oulu, 2000) p. 105.
[7] M. Valden, R.L. Keiski, N. Xiang, J. Pere, J. Aaltonen, M. Pessa, T. Maunula, A. Savimäki, A. Lahti and M. Härkönen, J. Catal. 161 (1996) 614.
[8] M.L. Unland, J. Catal. 31 (1973) 459.
[9] K. Rahkamaa, Licenciate Thesis (Åbo Akademi University, Turku, 2000) p. 77.
[10] G.I. Panov, A.K. Uriarte, M.A. Rodkin and V.I. Sobolev, Catal. Today 41 (1998) 365.
[11] X. Feng and W.K. Hall, J. Catal. 166 (1997) 368.
[12] H.Y. Chen and W.M.H. Sachtler, Catal. Today 42 (1998) 73.
[13] X. Feng and W.K. Hall, Catal. Lett. 41 (1996) 45.
[14] X. Feng and W.K. Hall, J. Catal. 166 (1997) 368.
[15] H.-Y. Chen and W.M.H. Sachtler, Catal. Lett. 50 (1998) 125.
[16] H.-Y. Chen and W.M.H. Sachtler, Catal. Today 42 (1998) 73.
[17] R.W. Joyner and M. Stockenhuber, Catal. Lett. 45 (1997) 15.
[18] G.I. Panov, V.I. Sobolev, K.A. Dubkov, V.N. Parmon, N.S. Ovanesyan, A.E. Shilov and A.A. Shteinman, React. Kinet. Catal. Lett. 61 (1997) 251.
[19] V. Sobolev, G. Panov, A. Kharitonov, V. Romannikov, A. Volodin and K. Ione, J. Catal. 139 (1993) 435.
[20] N.S. Ovanesyan, A.A. Shteinman, K.A. Dubkov, V.I. Sobolev and G.I. Panov, Kinet. Catal. 39 (1998) 792.
[21] W.K. Hall, X. Feng, J. Dumesic and R. Watwe, Catal. Lett. 52 (1998) 13.
[22] T.V. Voskoboinikov, H.-Y. Chen and W.M.H. Sachtler, Appl. Catal., B 19 (1998) 279.
[23] K. Lazar, A.N. Kotasthane and P. Fejes, Catal. Lett. 57 (1999) 171.
[24] A.V. Kucherov, C.N. Montreuil, T.N. Kucherova and M. Shelef, Catal. Lett. 56 (1998) 173.

[25] H.-T. Lee and H.-K. Rhee, Catal. Lett. 61 (1999) 71.

[26] R. Joyner and M. Stockenhuber, J. Phys. Chem., B 103 (1999) 5963.

[27] H.-Y. Chen, El.-M. El-Malki, X. Wang, R.A. van Santen and W.M.H. Sachtler, J. Mol. Catal., A: Chem. 162 (2000) 159

[28] O. Anunziata, A.R. Beltramone, Z. Juric, L.B. Pierella and F.G. Requejo, Catal. Lett. (2003) in press.

[29] F.G. Requejo, J.M. Ramallo-López, A.R. Beltramone, L.B. Pierella and O.A. Anunziata, Catal. Lett. (2003) in press.

[30] H.Y. Chen, X. El-Malki Wang, R.A. Van Santen and W.M. Sachtler, J. Mol. Catal. 162 (2000) 159.

[31] K.-I. Segawa, Y. Chen, J.E. Kubsh, W.N. Delgass, J.A. Dumesic and W.K. Hall, J. Catal. 76 (1982) 112.

[32] L. Lobree, I. Hwang, J. Reimer and A. Bell, J. Catal. 186 (1999) 242.

[33] J. Amiridis, F. Puglisi and J. Dumesis, J. Catal. 142 (1993) 572.

[34] K. Hadjiivanov, J. Saussey, J. Freyzs and J. Lavalley, Catal. Lett. 52 (1998) 103.